Potential and Limits of Dynamic Mechanical Analysis as a Tool for Fracture Resistance Evaluation of Isotactic Polypropylenes and Their Polyolefin Blends

C. Grein, K. Bernreitner, M. Gahleitner

Borealis GmbH, St.-Peter Strasse 25, A-4021 Linz, Austria

Received 27 February 2003; accepted 8 March 2004
DOI 10.1002/app.20606
Published online in Wiley InterScience (www.interscience.wiley.com).

ABSTRACT: Potential and limits of dynamic mechanical analysis (DMA) as a tool for fracture resistance evaluation of isotactic polypropylenes and their polyolefin blends are presented. A minimum of information about the materials under investigation is a prerequisite to interpret the DMA traces in a right way. Although DMA is, in general, a powerful method to rank materials in term of toughness, care should be taken with (1) nucleated materials (where both intensity and strength of molecular relaxations need to be taken into account in material evaluation) and with (2) visbroken (i.e., peroxyde treated) grades. Except for these cases, the strengths of the principal or secondary molecular relaxation evaluated by DMA and the Charpy impact toughness correlate quantitatively when all the grades of a series exhibit unstable crack propagation. When changes in the macroscopic mode of fracture or in blend morphology occur, only qualitative correlations remain possible. © 2004 Wiley Periodicals, Inc. J Appl Polym Sci 93: 1854–1867, 2004

Key words: poly(propylene) (PP); blends; relaxation; toughness

INTRODUCTION

Dynamic mechanical analysis (DMA) offers the possibility to obtain a unique fingerprint of (1) relaxations process, (2) modulus, and (c) damping factor of any polymer over a wide range of temperatures and/or frequencies in a couple of hours with several grams of material. Its potential as a macroscopic toughness indicator has already been mentioned in several studies. Quantitative or at least qualitative relationships between the strengths of the principal or secondary relaxations and the fracture resistances have been found,[1–12] although the small strain, linear viscoelastic measurements in DMA differ fundamentally to the large strain, nonlinear behavior observed under impact conditions.

To allow high levels of energy absorption, the molecular processes involved in the microscopic deformation (1) must have a lower relaxation time than the characteristic time of the external loading, and (2) must be numerous enough to play an effective role. In practice, for Charpy tests carried out at about 3.8 m/s and room temperature, a material will be ductile if it contains one (or more) subambient relaxation(s) and if the strength of this (these) relaxation(s) is (are) important enough. If not, it will be brittle. However, even in this case, a correlation between the strength of the molecular relaxations present in the system and toughness is expected.

In this article, the potential of DMA for rapid toughness characterization and material ranking will be highlighted for isotactic polypropylenes (iPP), random iPP copolymers with ethylene, and ethylene–propylene rubber-toughened iPP blends (iPP/EPR). Its limits for complex systems will also be shown.

Correspondence to: C. Grein (christelle.grein@borealisgroup.com).

Journal of Applied Polymer Science, Vol. 93, 1854–1867 (2004)
© 2004 Wiley Periodicals, Inc.

EXPERIMENTAL

DMA measurements

Experimental setup and samples

In DMA measurements a periodic stress, σ, (or strain, ϵ or γ) is applied to a solid sample and the resulting strain (or stress) is recorded. To avoid nonlinear responses and morphological changes induced by internal heat generation, measurements are carried out in a rather low frequency range (typically 0.01–20 s^{-1}), and applied stresses (or strains) are small.

Our conventional tests were performed in accordance with ISO 6721 with $50 \times 10 \times 1$ mm^3 compression moulded samples, as a function of temperature at 1 Hz with a heating rate of 1 K/min under free oscillation in torsional mode using a Myrenne ATM3 pen-

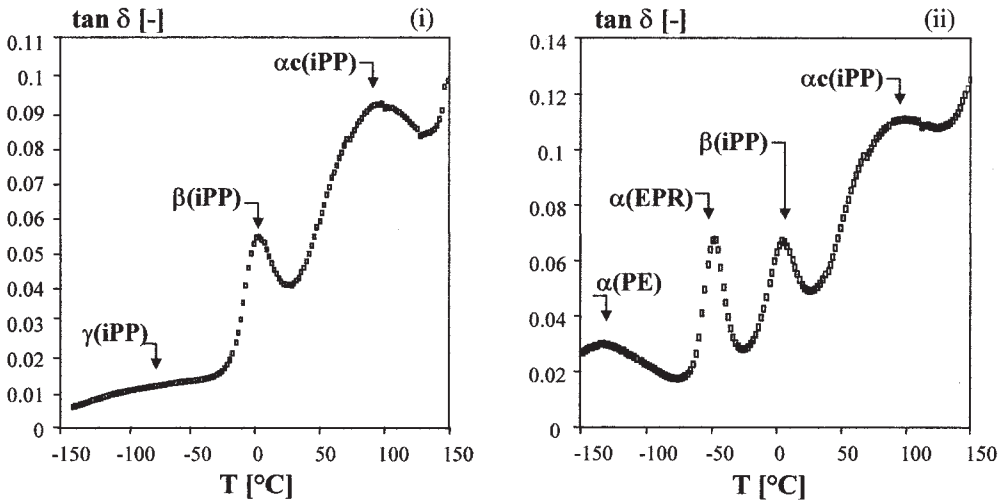

Figure 1 Molecular relaxations in (i) iPP and (ii) iPP/EPR blends as revealed by DMA traces (at a frequency of 1 Hz and a heating rate of 1 K/min).

dulum or at 1 Hz with a heating rate of 2 K/min under forced oscillation in a torsional mode with an RDS II (Rheometrics). With this latter apparatus, some measurements were performed with frequencies from 0.1 to 15 Hz and with heating rates in between 1 and 20 K/min. The (in phase) storage modulus, G', the (out of phase) loss modulus G'' and the damping factor, tan δ ($= G''/G'$) were recorded. Because tan δ is dimensionless, it provides a convenient measure to compare polymers where G' and G'' may be subjected to changes because of alterations in composition, geometry, or process parameters. Sepe has defined it as "an index of viscoelasticity."[13]

Transitions in iPP and iPP/EPR blends

Figure 1(i) shows a typical DMA curve for an iPP. Three transitions can be distinguished:[14,15]

1. the α_c-transition at 80°C, accounting for polymer rearrangements. It is assumed to have its origin in the diffusion of conformational defects in the crystalline phase to the crystalline–amorphous interphase. Both amorphous and crystalline phases are therefore thought to be affected by this transition;
2. the β-transition or glass transition at about 0°C for the amorphous parts of the semicrystalline iPP;
3. the γ-transition at −80°C of weak intensity attributed to local motions of long $(CH_2)_n$ segments, included in the iPP macromolecules as internal defects.

In addition, an iPP/EPR blend exhibits at least one more transition [Fig. 1(ii)]: the glass transition of the amorphous EPR (ethylene propylene rubber) at about −50°C. A transition at −120°C can sometimes also be seen accounting for the glass transition of PE. This is especially the case for ethylene-rich rubbers polymerized *in situ* [Fig. 1(ii)]. Even more transitions can occur in complex materials with several elastomeric phases.

Procedure for evaluating the strength of the molecular relaxations

Figure 2 illustrates the procedure used to evaluate the amount of molecular motions activated during loading. It is based on the idea that the strengths of the relaxations, characterized by the areas under the tan δ

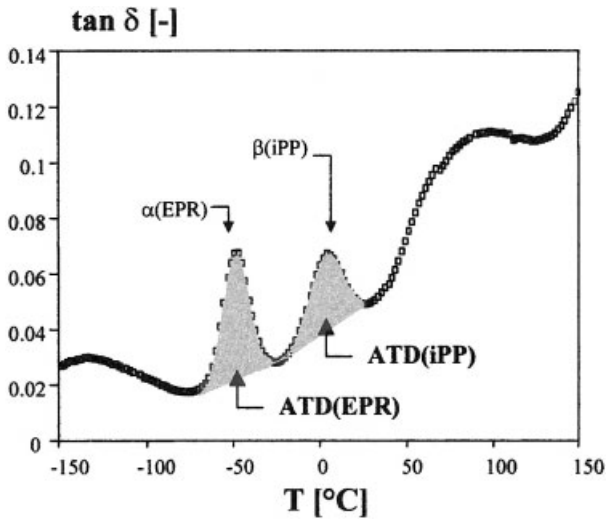

Figure 2 Procedure used to calculate the relaxation strengths of both matrix [ATD(iPP)] and rubber phase [ATD(EPR)].

peaks, plotted against frequency and temperature, are direct indicators of the damping behavior of a given material. Assuming an approximate time–temperature equivalence, a positive correlation is thus expected between impact toughness and strength:

1. of the tan δ peak of the β-relaxation of iPP [i.e., the area under the tan δ peak at ~0°C, called ATD(iPP)] for homopolymers, accounting for the molecular mobility of the matrix;
2. of the tan δ peak of the α-relaxation of EPR [i.e., the area under the tan δ peak at ~−50°C, called ATD(EPR)] for the elastomer-modified iPP, accounting for the molecular mobility of the elastomer particles. Indeed, because a high testing speed corresponds to high frequencies (nonmeasurable, assumed to be around 10^5–10^6 Hz), the latter are first activated under impact conditions.

To use a uniform data reduction procedure, the areas under the damping peaks were delimited between the adjoining minima, as suggested by most of the studies dealing with impact strength–damping factor correlations. In the following, relative units proportional to Kelvins will be used to characterize the strengths of both relaxations. Except for some indicated cases, the reported data have been calculated using a coherent unit system, and can be compared among themselves independent of the series.

To avoid confusion, it should be pointed out that "strength" in connection with DMA traces will refer in this study exclusively to the areas under the relaxation peak (i.e., their magnitude), not the heights of these peaks (i.e., their amplitude). This way, the whole relaxation spectrum is taken into account in material evaluation. ATD(iPP) and ATD(EPR) should therefore reflect the contributions and distributions of all structural groups present in the material, and not be punctual parameters extracted from relaxation maxima.

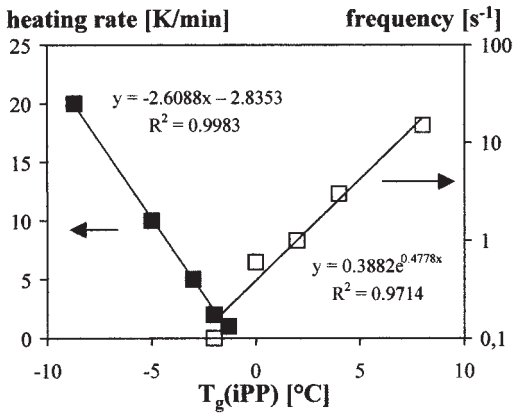

Figure 3 Evolution of T_g [ATD(iPP)] with to heating rate and frequency for a standard iPP.

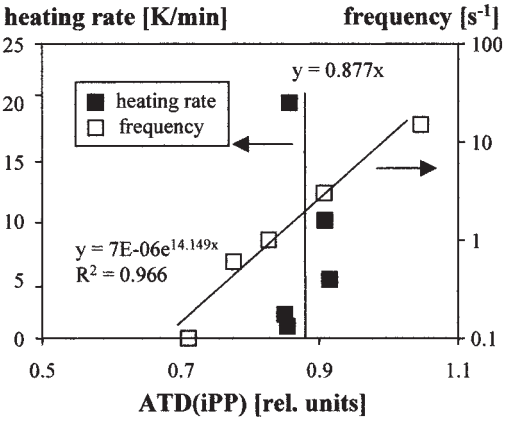

Figure 4 Sensitivity of β-relaxation strengths [ATD(iPP)] to heating rate and frequency for a standard iPP.

Mechanical testing

Notched Charpy impact tests were performed at 3.8 m/s according to ISO 179-2/1eA on injection-molded specimens of 80 × 10 × 4 mm^3 at 23 and −20°C. All the materials were molded under the same standard conditions. The parts were not conditioned prior to testing, which was done at least 96 h after molding.

Ductile–brittle transitions were occasionally determined to get a deeper insight on the fracture behavior of a grade over a wide range of temperature. Measurements were carried out on an instrumented Charpy device (Roell Amsler RKP 50, instrumented by HKE) with 50 J pendulum and a test speed of 1.5 m/s using SENB (single etched notched bending) specimens (a/W = 0.25) following ISO 179. A sharp incurvate in the plot $G_{tot} - T$ (with G_{tot} being the fracture energy) was associated with the temperature at which the ductile–brittle transition occurred.

Materials

The investigated grades were experimental or commercial products from Borealis. In each series, the materials were polymerized in the same way using coherent reactor settings (same catalyst, same external donor, same TEAL/external donor ratios, etc.). In each series, they were compounded on the same extruder using identical extruder settings (temperature profile, screwspeed, etc.). The stabilization recipe was the same for each series.

TABLE I
Comparison of Strengths of Matrix Molecular Relaxations, ATD(iPP), with Notched Impact Strengths, NIS, of an Homopolymer and a Rubber-Modified iPP/EPR as a Function of the Annealing Temperature

Annealing temperature	23	80	110	140	°C
ATD(iPP)—iPP	0.47	0.499	0.559	0.629	rel. units
$NIS_{23°C}$—iPP	2.7	2.1	2.2	2.9	kJ/m^2
ATD(iPP)—iPP/EPR	0.292	0.327	0.414	0.509	rel. units
$NIS_{23°C}$—iPP/EPR	9.5	9	9.8	17.2	kJ/m^2
$NIS_{-20°C}$—iPP/EPR	4.1	4.7	5.5	7.3	kJ/m^2

The strength of the rubber relaxation in the iPP/EPR system was constant.

RESULTS

Sensitivity of ATD towards some external parameters

Sensitivity of ATD towards test variables

Due to their inherent viscoelastic character, iPP and iPP/EPR blends exhibit frequency and heating rate-dependent responses to external loading. Figure 3 shows for an iPP with a melt flow rate (MFR) of 0.2 g/10 min the evolution of T_g taken as the maximum of the β-relaxation peak of iPP vs (1) frequencies in between 0.1 to 15 Hz, and (2) heating rates in between 1 and 20 K/min. As expected, the higher the frequency, the higher T_g as the time to accommodate an external load is shortened. Moreover, the lower the heating rate, the higher the T_g. The sensitivity of the evaluated strengths of the β-relaxation as a function of (1) frequency and (2) heating rate is shown in Figure 4(i) and (ii). Whereas the recorded strengths are only a little dependent on the heating rate with a value of 0.877 $\pm$ 0.028, they increase linearly with the logarithm of the frequency within the investigated range, resulting from a broadening of the β-relaxation peak with increasing frequency. The ATD of various materials can therefore only be compared when the set frequencies are identical. In practice, a frequency of oscillations of 1 Hz is recommended by international standards (ASTM D4065-94, ISO 6721).

Sensitivity of ATD towards annealing

Annealing is well known to have a positive influence on toughness when the annealing temperature, T_{ann}, is high enough to induce significant changes in the microstructure of the investigated materials.[16–20] According to several studies using different methods of mechanical characterization (EWF, J-Integral, conventional Charpy measurements), this latter temperature is about 110–120°C.[16–20] Above it, the higher T_{ann} ($<T_{melting}$), the better the mechanical performance in terms of toughness, at least up to a temperature where the material starts to melt on a bigger scale. In this zone, partial melting and recrystallization processes are suggested to promote the development of thin crystallites and a rearrangement of noncrystallized macromolecules. Table I compares toughness and ATD(iPP) values for both homopolymer (Borealis' K2XMOD) and rubber-modified iPP/EPR blend (Borealis' MC15XMOD) annealed at 80, 110, and 140°C for 168 h. Except for the nonannealed reference (sample

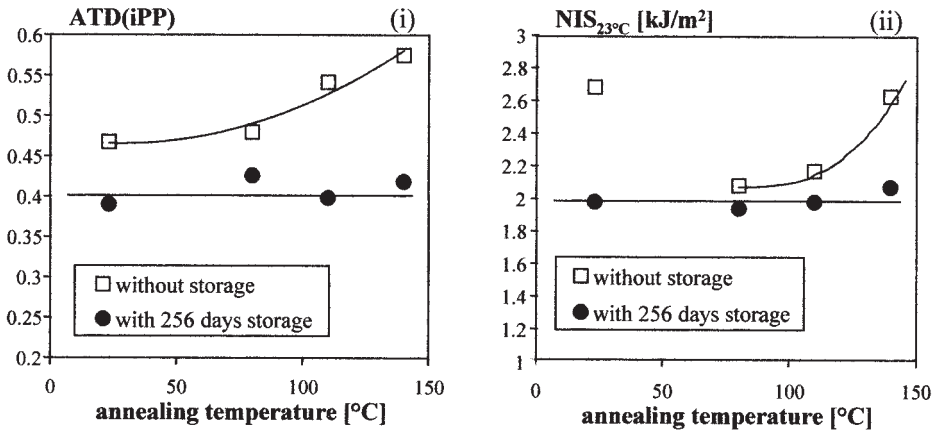

Figure 5 Influence of physical aging (256 days, room temperature) on (i) matrix relaxation strengths [ATD(iPP)], and (ii) fracture toughness measured at room temperature (NIS) as a function of annealing temperature for an iPP (Borealis' K2XMOD). Note the parallel evolution of ATD(iPP) and NIS.

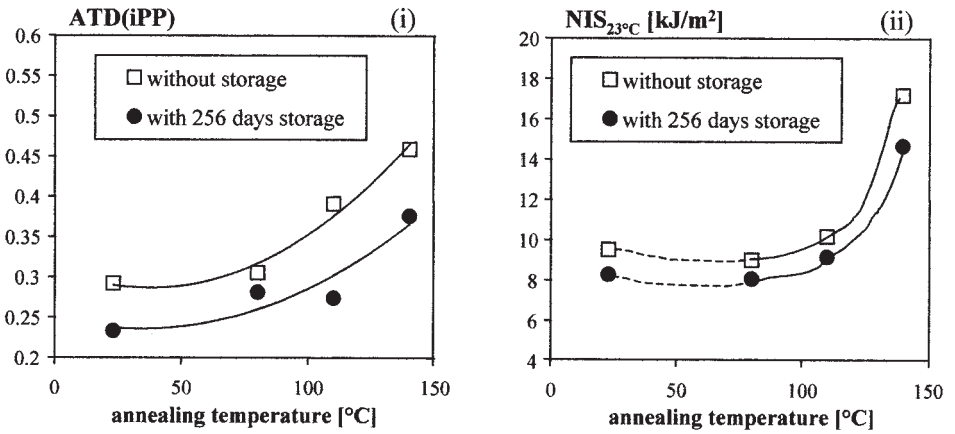

Figure 6 Influence of physical aging (256 days, room temperature) on (i) matrix relaxation strengths [ATD(iPP)], and (ii) fracture toughness measured at room temperature (NIS) as a function of annealing temperature for an iPP/EPR blend (Borealis' MC15XMOD). Note the parallel evolution of ATD(iPP) and NIS.

stored 4 days at 23°C), the mechanical strengths measured at room temperature correlate qualitatively with the amount of matrix molecular relaxations estimated by DMA. A quantitative correlation between both parameters for all test conditions (including reference) could only be found for ATD(iPP), and the fracture resistance measured at −20°C following the equation NIS = 11.2ATD(iPP) + 1 (R^2 = 0.961).

Sensitivity of ATD towards physical aging

To check the influence of physical aging on the micromechanical response of polypropylenes, the same materials as above were investigated. However, instead being annealed for 168 h, they were annealed for 24 h (at 80, 110, and 140°C), and stored at room temperature for 256 days. As obvious from Figures 5 and 6, the lowering of impact toughness for physically aged samples was reflected by the ATD(iPP) values for both systems and all test conditions. Moreover, for the homopolymer, the erasure of the annealing benefits after 9 months of storage in terms of toughness (NIS ≈ 2 kJ/m^2) was suggested by the constance of ATD(iPP) over the annealing temperatures (Fig. 5). Such a strong correlation, however, could not be found for the iPP/EPR blend, where both evolutions of the amount of the matrix β-relaxation and fracture resistance in the function of the annealing temperature exhibit only the same trends (Fig. 6).

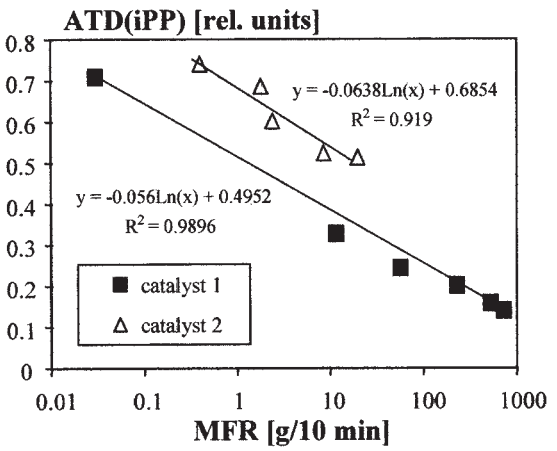

Figure 7 Evolution of ATD(iPP) with the logarithm of MFR for iPP produced with two different catalysts.

Case of iPP homopolymers

Figure 7 shows the evolution of the magnitude of the β-relaxation of iPP homopolymers over a wide range of MFR for two different catalyst systems. The different responses of both series towards small strain deformations are highlighted. This is a direct consequence of different molecular structures (stereoregularity, lamella thickness, etc.) achieved by modifying the polymerization conditions: the series with the lower ATD was that with the higher Young moduli ($E_{high} \approx E_{low}$ + 400 MPa, both series being nonnucleated).

TABLE II
Evolution of the Matrix Molecular Relaxations, ATD(iPP), Notched Impact Strengths, NIS, at Room Temperature and Unnotched Impact Strengths, IS, at −20°C towards the MFR

MFR	0.4	1.8	2.4	8.5	19.6	g/10 min
ATD(iPP)	0.741	0.686	0.602	0.523	0.513	rel. units
$NIS_{23°C}$	7.2	5.9	4.3	3.1	2.1	kJ/m^2
$IS_{-20°C}$	23.5	20.9	17.8	15.5	14	kJ/m^2

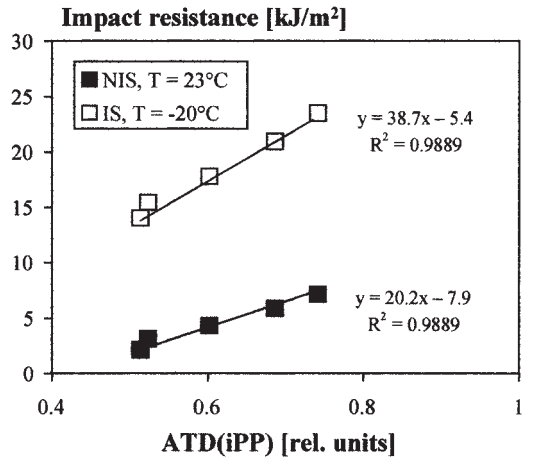

Figure 8 Linear correlation between impact strength and relaxation strengths for a series of iPP with different MFR.

As is obvious from Table II, an MFR increase has a detrimental effect on the damping capacities of a material due to the lowering of inter- and intralamellar link densities. When all materials broke in a brittle way (see raw data in Table II), this was reflected in a linear decrease of the toughness at 23 and −20°C towards the logarithm of MFR following: NIS = −1.33ln(MFR) + 6 with R^2 = 0.957 for notched specimens tested at 23°C; and IS = −2.52ln(MFR) + 21.2 with R^2 = 0.947 for unnotched samples tested at −20°C.

Moreover, as suggested by Figure 8, there is a 1 : 1 correlation between the notched impact strengths at 23°C (resp. the unnotched impact strengths at −20°C) and the amount of motions activated at T_g. Prediction of the toughness knowing the ATD (and vice versa) therefore appears to be possible when a calibration curve can be produced (within the limits, which will be discussed latter on).

Case of ethylene/propylene (EP) random copolymers

Random E/P copolymers consist of PP chains in which small amounts of ethylene (C_2) are quite randomly distributed. The incorporation of C_2 reduces the overall crystallinity of the polymer; the C_2 units act as defects for the regularity of chain configuration, and thus promote plastic deformation. The room temperature fracture toughness increases with the C_2 content, as illustrated in Figure 9(i), for E/P random copolymers 9(ii) having an MFR of about 8 g/10 min. Three domains can roughly been distinguished as a function of C_2: (1) up to 6 wt % the impact resistance increases linearly with the C_2 content; (2) at about 7 wt % of C_2 a brittle to ductile transition occurs; (3) above 7 wt % of C_2, the materials exhibit a ductile behavior.

These results are qualitatively in agreement with the ranking provided by the estimation of the strengths of the molecular motions activated when the sample is submitted to an external load: the areas under the β-relaxation peak evolve in a parabolic way with the C_2 content [Fig. 9(i)]. However, there is no quantitative correlation between NIS measured at room temperature and DMA related data (Fig. 10), illustrating that these latter cannot predict changes of macroscopic behavior in one series. This is actually not surprising because:

1. recorded macroscopic values at 23°C are punctual values and do not reflect the entire behavior of a given material as a function of temperature or test speed (especially not the ductile–brittle transition values). This remark is actually valuable for all polypropylene families (and for all other polymers!);
2. the T_g of the PP/PE randoms is not independent of the C_2 content. It decreases with increasing amounts of C_2. In our series, its evolution could

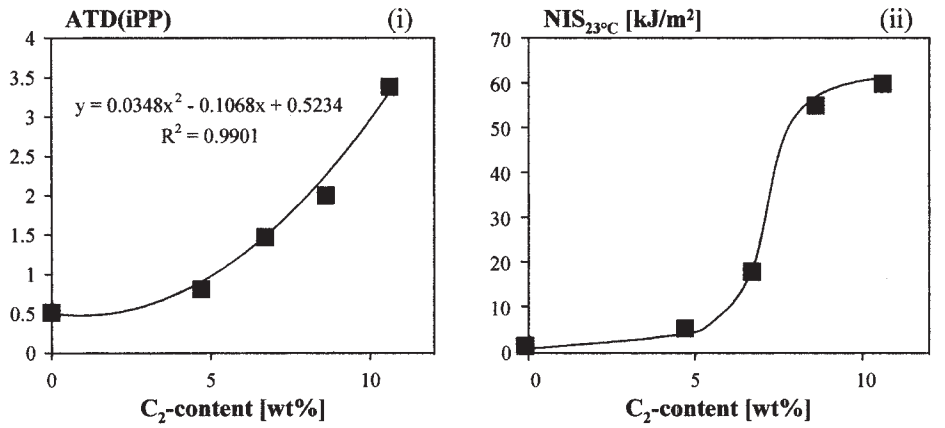

Figure 9 Evolution of (i) ATD(iPP) and (ii) notched impact strengths (NIS) measured at 23°C with the C_2 content for random copolymers.

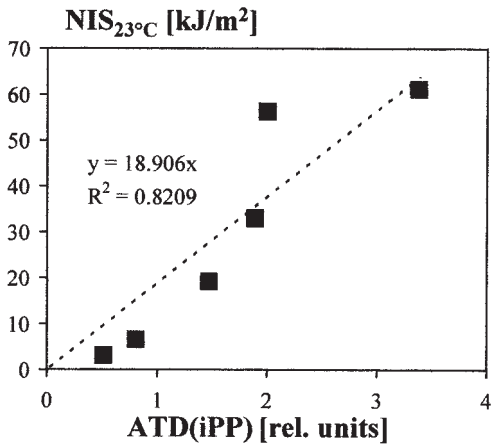

Figure 10 Matrix relaxation strength [ATD(iPP)] plotted vs impact resistance (NIS) measured at 23°C for a series of random copolymers with different C_2-contents. Note the qualitative correlation between both parameters.

be described with the equation $T_g = -0.0805C_2^2 - 0.9421C_2 + 4.0041$ ($R^2 = 0.9967$);

3. changes in phase morphology (up to an onset of phase separation) might occur as a function of C_2 content.

Further investigations are under way to clarify the respective influence of these aspects on the evolution of ATD(iPP). From this perspective it would be particularly interesting to compare the ATD(iPP) with the temperature (resp. test speed) at which ductile–brittle transitions occur at a given test speed (resp. temperature) over a wide range of temperatures (resp. test speed).

Case of heterophasic iPP copolymers with a random EP or a PP matrix (RAHECO–HECO)

The rubber phase is, in a first approximation, responsible for the toughness of heterophasic iPP because the particles act (1) as initiators of the damage mechanics through particle cavitation—because of their role of stress concentrators, which also promote matrix plastic flow, and (2) as stabilizers of the deformed polymer by a mechanism of crazing.[21,22] The strength of the molecular relaxation corresponding to the dispersed phase [ATD(EPR)] is therefore expected to correlate with the macroscopic behavior of these materials.[1–3]

The use of DMA-related parameters will be first demonstrated with three independent series of heterophasic iPP copolymers having an MFR(230°C, 2.16 kg) = 8 for which the rubber content has been varied systematically. Materials differ in between a series in terms of molecular characteristics of their elastomeric phase and amount of C_2 in their matrix (S-1 are HECOs, S-2 are RAHECOs with 4 mol % C_2 in the continuous phase, S-3 are RAHECOs with 8 mol % C_2 in the continuous phase). Some of the mechanical characteristics of the studied grades measured at 23°C are given in Table III. Further details can be found in refs. 23 and 24. According to impact measurements (notched impact strengths, NIS, measured at 23°C) the grades ranked as follows: S-3 > S-2 > S-1. As is obvious from Figure 11, the excellence of S-3 in terms of toughness could have been deduced directly (i.e.,

TABLE III
Some Mechanical Features of the Three Investigated Series of Copolymers at 23°C

Material	S1-1	S1-2	S1-3	S1-4	S1-5	S1-6	S1-7	S1-8		
%EPR	0	1	5	15	20	30	45	50		wt %
$NIS_{23°C}$	3.4	2.8	3.8	4.3	4.5	6.7	70	72		kJ/m^2
E_{flex}	1600	1470	1397	1080	1068	950	652	618		MPa
$\sigma_{3.5\%}$	42.4	37.5	35.8	28.3	27.3	23.5	15.7	14.5		MPa
Material	S2-1	S2-2	S2-3	S2-4	S2-5	S2-6	S2-7	S2-8	S2-9	
%EPR	0	2.3	4.6	8	11.5	14.9	18.4	20.7	23	wt %
$NIS_{23°C}$	4.8	6.3	6.7	8.1	9.8	11.4	14.7	16.3	19.5	kJ/m^2
E_{flex}	1009	899	861	798	745	686	641	589	586	MPa
$\sigma_{3.5\%}$	27.1	24.2	23	21.3	19.7	18.2	16.8	15.4	15.3	MPa
Material	S3-1	S3-2	S3-3	S3-4	S3-5	S3-6	S3-7	S3-8	S3-9	
%EPR	0	3.5	6.9	12.1	17.2	22.4	27.6	31	34.5	wt %
$NIS_{23°C}$	7.6	9.4	11.4	16.6	54.6	68.4	70.3	70.6	69	kJ/m^2
E_{flex}	730	697	652	583	514	459	401	363	329	MPa
$\sigma_{3.5\%}$	21.9	19.1	17.8	16	14.1	12.5	10.8	9.9	8.9	MPa

NIS: notched impact strength (measured according to ISO179/1eA); E_{flex}: flexural modulus (measured according to ISO 178); $\sigma_{3.5\%}$: stress at 3.5% measured on bending tests according to ISO 178.

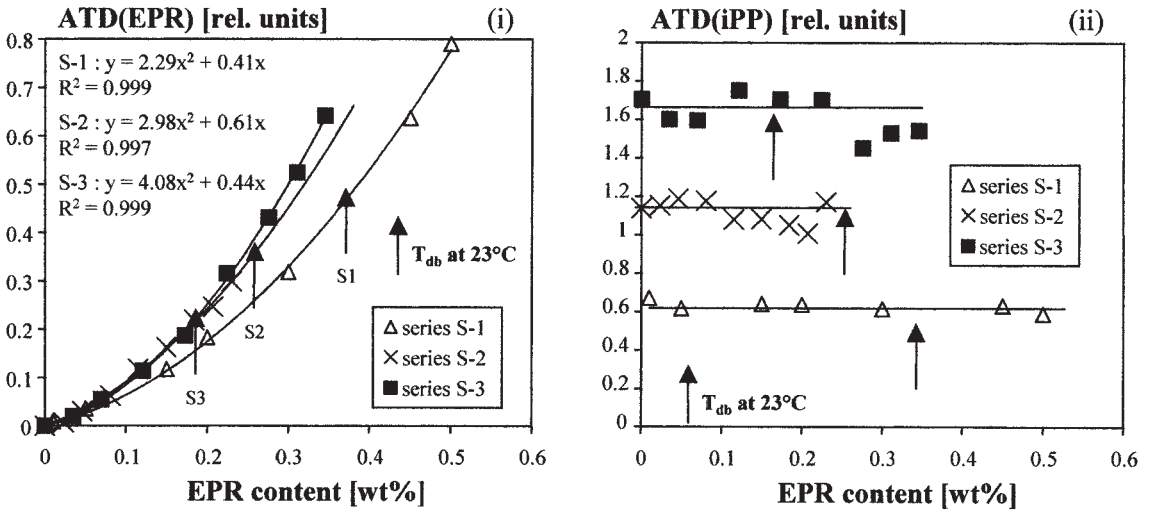

Figure 11 Evolution of the relaxation strengths of (i) the rubber phase, and of (ii) the matrix as a function of the rubber content for three independent series of iPP/EPR blends. The arrows on the figure indicate the amount of rubber neceassary at 23°C under impact conditions to pass from a brittle behavior to a ductile behavior.

without impact testing) with molecular relaxation considerations. At given rubber content: (1) S-3 and S-2 have a more mobile elastomer phase than S-1. Therefore, S-3 ≈ S-2 > S-1; (2) S-3 has a more mobile matrix than S-2 (ATD(iPP-S3) > ATD(iPP-S2), leading to S-3 > S-2). For these grades it is also interesting to note that the strengths associated with the matrix do not change with the rubber content.

Another example for the use of DMA as tool for toughness assessment is given in Table IV. Two developmental materials that differed in their rubber and talc contents showed identical conventional NIS values at both 23 and −20°C. They could only have been mechanically distinguished by the determination of their ductile–brittle transition, T_{db}, which required a rather time-consuming temperature screening (in this case the tests were performed from −60 to 100°C with a constant test speed of 1.5 m/s). With this method, a lower temperature at which the ductile–brittle transition occurs indicates a tougher material. Comparison and analysis in terms of ATD of the DMA curves confirmed within a couple of hours the material ranking obtained with extensive mechanical testing.

A last example is a model series, presented in Table V, consisting of seven iPP/EPR reactor blends with EPR intrinsic viscosities (IV) varying from 1.7 to 6 dL/g while all other parameters are kept constant (IV is a parameter proportional to average molecular weight).[25] A linear increase of (1) toughness (in standard Charpy tests performed at 23°C) and of (2) ATD(EPR) were observed with increasing IV on a logarithmic scale (Fig. 12). The strong linear correlation observed between the fracture resistance and ATD(EPR) in Figure 13 suggests energy absorption to be predominantly controlled by the molecular weight (M_w) of the dispersed phase. This conclusion is coherent with the fact that higher amounts of molecular entanglements in the amorphous elastomer and tie-molecules between the crystalline parts are present in systems with high molecular weights. As we will see in the next section, it constitutes only part of the truth.

In addition, it should be pointed out that even a rough estimation of the mechanical performances of an unknown iPP/EPR blend is impossible using DMA as unique test method. As it has been demonstrated, ATD(EPR) is (at least) a function of M_w and the volumetric fraction of the dispersed phase.

TABLE IV
Comparison of (i) the Conventional Mechanical Performance (Notched Impact Strengths, NIS, at −20 and 23°C), of (ii) the "Advanced" Mechanical Performance (Temperature at Which the Ductile–Brittle Transitions, T_{db}, occur) and of (iii) the Micromechanical Responses (ATD(EPR) and ATD(iPP)) of Two Underdevelopment Materials

	$NIS_{23°C}$ (kJ/m²)	$NIS_{-20°C}$ (kJ/m²)	ATD(EPR) (rel. units)	ATD(iPP) (rel. units)	T_{db} (°C)
M-1	35	6	0.626	0.226	−3
M-2	33	6	0.472	0.262	13

TABLE V
Evolution of (i) Charpy Toughness at Room Temperature ($NIS_{23°C}$), (ii) Average Molecular Weight in Number, M_n, and in Weight, M_w, and (iii) Average Particle Diameter in Number, D_n, and in Weight, D_w, as a Function of the Intrinsic Viscosity, IV, of the Investigated iPP/EPR Blends

IV	1.7	2.1	2.7	3	3.9	4.7	6	dL/g
$NIS_{23°C}$	4.5	6	7.7	9.4	10.8	11.8	12.9	kJ/m^2
Rubber M_n	56	84	93	102	128	112	180	kg/mol
Rubber M_w	233	320	412	530	706	145	1200	kg/mol
Rubber D_n	0.74	1.07	1.41	1.41	1.37	1.32	1.04	nm
Rubber D_w	0.93	1.57	1.96	1.82	1.77	1.67	1.29	nm

Note the quantitative correlation between IV and M_w, $M_w = 237\ln(IV) - 200$ with $R^2 = 0.970$.

LIMITS IN DMA-IMPACT STRENGTHS CORRELATIONS FOR COMPLEX POLYMER SYSTEMS

Morphological effects in heterophasic copolymers

As highlighted earlier, DMA is able to reveal polymer changes at the micro- to nanoscale: variations in M_w or rubber amount can be followed. What about elastomer morphology, a parameter that is known to have a determining influence on the fracture toughness? There is theoretically no clear answer. On the one hand, because DMA deals with molecular motions, changes in particle sizes should not be seen. On the other hand, particles interact with their surrounding environment: their DMA trace could be influenced by the size of the matrix ligaments around them.

To clarify this issue, we again consider the series of iPP/EPR blends with various IV investigated earlier. As reported in Table V, both elastomer M_w and particles diameters do not vary in the same direction over the IV range. This result was actually expected because the morphology of the dispersed phase in heterophasic copolymers is mainly controlled by the viscosity ratio between rubber and matrix.[25] Obviously, there is no correlation between the particle size and a material relaxation [neither ATD(EPR) nor ATD(iPP)] as illustrated by Figure 14: DMA traces do not reflect particle size variations.

In addition, to elucidate whether M_w or elastomer morphology mainly controls the mode of fracture of the materials, the ductile–brittle transitions were recorded at fixed test speed over a wide range of temperatures for materials with IV = 1.7, 3, and 6. It was shown that despite decreasing with increasing the rubbery IV, the temperature at which the ductile–brittle transitions, T_{db}, occurred did not correlate *linearly* with the logarithm of the intrinsic viscosity of the rubber.[25] In other words, although providing the right material ranking, the amount of elastomer molecular relaxations only correlates qualitatively with T_{db}, suggesting once more these molecular motions not to reflect particle size changes, as shown by Figure 15.

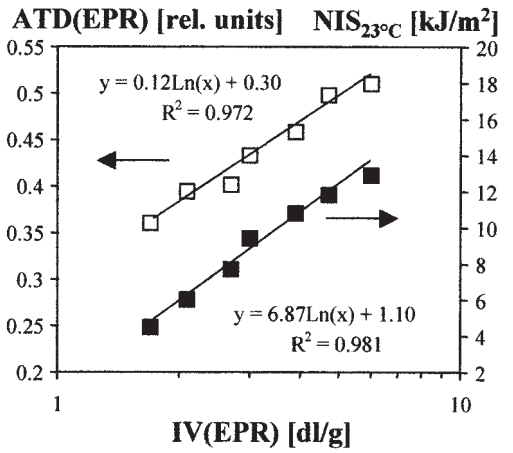

Figure 12 Evolution of the relaxation strength of the rubber phase [ATD(EPR)] and of the Charpy notched impact resistance (NIS) at 23°C towards the logarithm of the intrinsic viscosity (IV) in an iPP/EPR series where the IV was varied selectively, keeping all other parameters (including matrix MFR) constant.

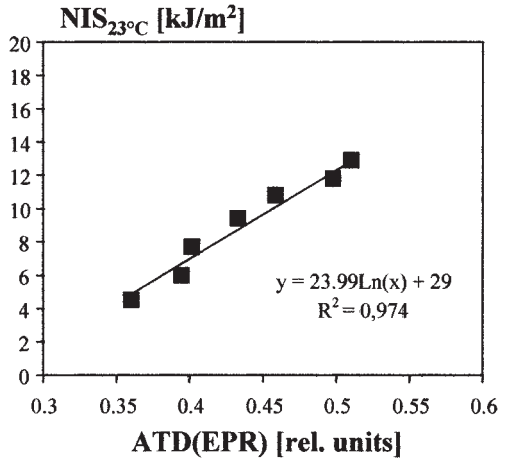

Figure 13 Quantitative correlation between the relaxation strengths of the rubber phase and the Charpy notched impact notched resistances (NIS) at 23°C for an iPP/EPR series where the EPR intrinsic viscosity (IV) has been varied selectively, all other parameters (inclusive matrix MFR) having been kept constant. Note that the grades failed in a brittle way.

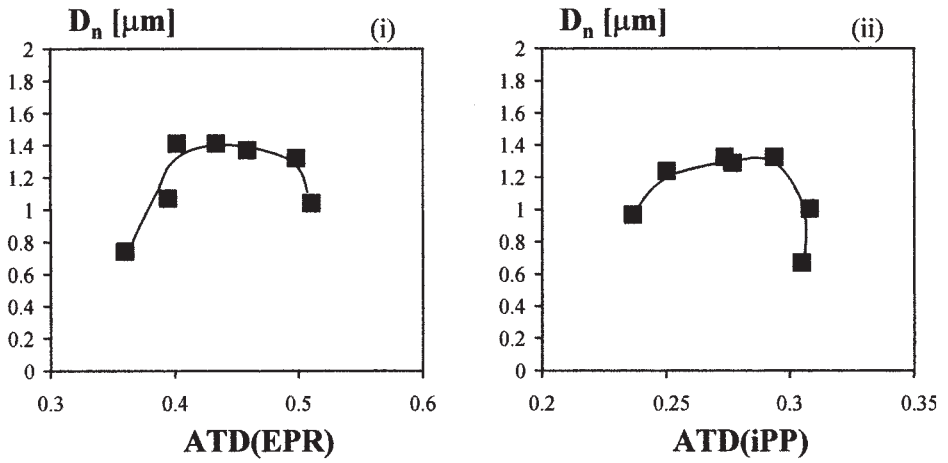

Figure 14 Evolution of the particle diameter, D_n, with (i) ATD(EPR) and with (ii) ATD(iPP) for an iPP/EPR series where the EPR intrinsic viscosities (IV) have been varied selectively all other parameters (inclusive matrix MFR) having been kept constant.

Combining the results of this section and an earlier leads to following conclusions: (1) ATD(EPR) reflects elastomer M_w, not particle sizes; (2) ATD(EPR) cannot predict quantitatively T_{db}; (3) in the *brittle mode of failure* (which corresponds in this example to NIS from 2 to 14 kJ/m^2), ATD(EPR) and fracture resistance correlate quantitatively, suggesting the particles to be "frozen" and to absorb energy that cannot be transferred to the matrix.

Therefore, for heterophasic systems, where both particle sizes and rubber molecular weights vary in a concomitent way, the use of rubber molecular relaxations to get precise information about mechanical characteristics is possible to a limited extent only.

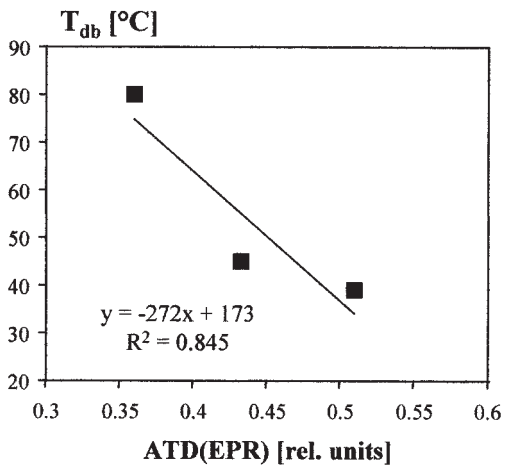

Figure 15 Qualitative correlation between ductile–brittle transitions and relaxation strengths of the included phase for an iPP/EPR series where the EPR intrinsic viscosities (IV) have been varied selectively, keeping all other parameters (including matrix MFR) constant.

Visbroken materials

In visbreaking of PP, a controlled amount of peroxide is added to the polymer in an extrusion step with the target of achieving a material with higher flowability and narrow molecular weight distribution. In the case of heterophasic EP copolymers, this may result in a partial crosslinking of the elastomeric phase. In any case, the viscosity ratio between this phase and the matrix will change as a result of the different reactions to radical attack induced by the peroxide. This, in turn, leads to a coarsening of the phase structure, the elastomer particles becoming bigger with increasing MFR.

Figure 16 shows the evolution of impact toughness and matrix molecular mobility for a series of visbroken homopolymers originating from a reactor iPP with MFR = 0.2 g/10 min. Obviously, there was no correlation between both parameters, ATD(iPP) being insensitive to changes in MFR. Considering the excellent correlation between macro- and micromechanical descriptors for nonvisbroken samples (see earlier), this result is a surprise. We are not able to explain it up to now: with the exception of a (limited) lowering of the damping capacity between −40 and −20°C (Fig. 17), the traces tan δ − temperature were nearly superimposable: neither the α_c-relaxation nor the T_g were influenced to a large extent by visbreaking. Because the ratio of the crystalline/amorphous phase has a nonnegligable influence on the DMA response of iPP, changes in the degrees of crystallinity, X_c, were suspected.[14,15] This assumption was, however, not confirmed by Differential Scanning Calorimetry (DSC), thermograms (using a +10/−10/+10 K/min heating/cooling program): for all the samples X_c was about 50 ± 1% (assuming a 100% crystalline phase to

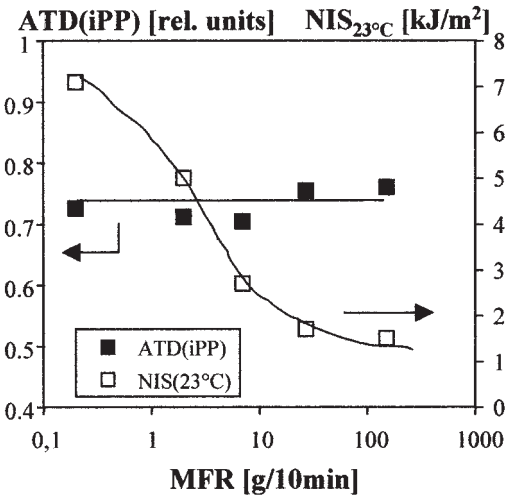

Figure 16 Evolution of the relaxation strengths of the main relaxation [ATD(iPP)] and of the Charpy notched impact resistances (NIS) at 23°C towards the logarithm of the MFR for visbroken homopolymers going from a base iPP with MFR = 0.2.

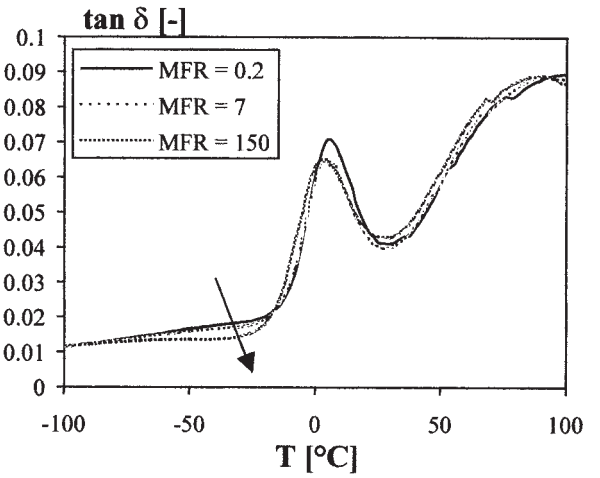

Figure 17 DMA traces for visbroken iPP (MFR = 7 and MFR = 150) and for the original nonvisbroken base grade (MFR = 0.2).

have a melt enthalpy of 207 J/g). From these DSC curves, variations of melt temperature or crystallization temperature could also be excluded. However, Gel Permeation Chromatography (GPC) measurements (Table VI) seem to indicate the presence of some long chains in the structure of high MFR grades as suggested by the M_z and M_z/M_w values. In particular, the increase of M_z/M_w for iPP with MFR = 27 and 150, while it was expected to lower continuously, is an indication for an inhomogeneous visbreaking process. This was confirmed by melt rheology (tests carried out at 230°C on a SR200 using ISO 6721): the plateau for low frequencies (ω = 0.1 rad/s) for grade with MFR = 150, being the fingerprint of such long macromolecules (Fig. 18). A possible consequence of this chain inhomogeneity may be the buildup of different crystalline structure in terms of lamellae size and lamellae size distribution for the different visbroken samples studied. This affirmation is, however, speculative, and should be verified (or falsified) by adequate test methods (Small Angle X-ray Scattering, Atomic Force Microscopy, etc.).

Similar difficulties (noncorrelation mechanics—DMA) arise from measurements carried out on heterophasic copolymers with both standard and random matrix. Therefore, DMA traces, performed using the experimental setup described above, appeared to be unsuitable in revealing changes induced by peroxide degradation.

Nucleated grades: Some restrictions in determination of ATD

To use a coherent data reduction procedure, the areas under the damping peak were delimited between the adjoining minima, as suggested by most of the studies dealing with impact strength-damping factor correlations. Although it has often proven its predictive ca-

TABLE VI
Main Characteristics of Visbroken iPP (MFR = 1, 7, 27, and 150 g/10 min) Originating from the iPP with an MFR = 0.2 g/10 min

MFR (g/10 min)	XCS (wt%)	$NIS_{23°C}$ (kJ/m^2)	ATD(iPP) (rel. unit)	ATD($T_{\alpha c}$) (rel. unit)	M_n (kg/mol)	M_w (kg/mol)	M_z (kg/mol)	M_w/M_n (−)	M_z/M_w (−)
0.2	2.2	7.1	0.725	1.364	175	1035	5804	5.9	5.6
1	2.8	5	0.712	1.564	154	792	3759	5.1	4.7
7	3	2.7	0.704	1.521	121	373	1040	3.1	2.8
27	3.5	1.7	0.755	1.463	87	215	1001	2.5	4.7
150	3.9	1.5	0.760	1.364	87	149	826	2.1	5.5

XCS: xylene cold soluble. ATD($T_{\alpha c}$): area under the αc-relaxation (limits: both adjoining minima) evaluated from DMA traces. Note that ATD($T_{\alpha c}$) is not sensitive to changes in MFR. M_n, M_w, M_z determined by Gel Permeation Chromatography (Waters 150°C, at 135°C using trichlorobenzene as solvant, M_n: average molecular weight in number, M_w: average molecular weight in weight, M_z: average molecular weight in volume).

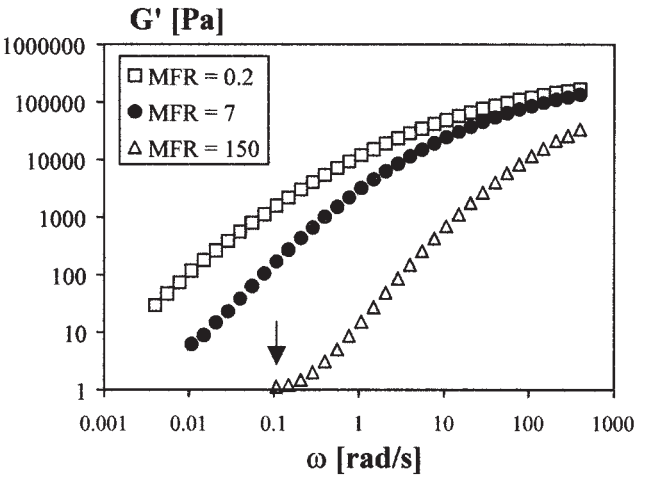

Figure 18 Shear stress, G', plotted against the logarithm of the frequency for visbroken iPP (MFR = 7 and MFR = 150) and for the original nonvisbroken grade (MFR = 0.2). The arrow indicates the presence of long chains in high flowable iPP.

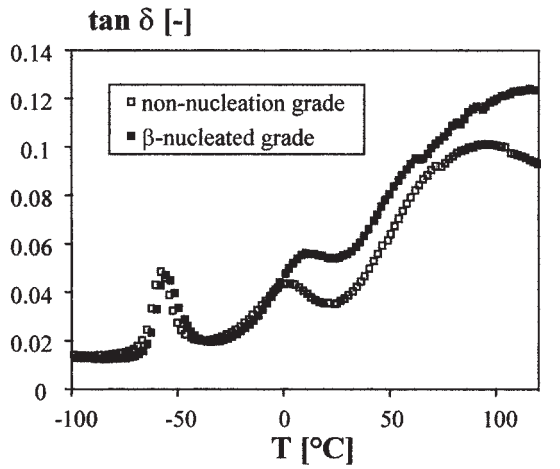

Figure 19 DMA traces for both nonnucleated and β-nucleated iPP/EPR blends.

pability, this way to estimate ATD might be deceptive in some cases. A typical example is that of β-nucleated materials, where care should be taken in interpreting isolated results. Fracture resistances measured at 23°C and "standard" ATD calculated for a nonnucleated series (that with the different intrinsic viscosities at given matrix MFR) and its β-nucleated homolog are reported in Table VII. As expected, the damping capacities of the rubber phase were not affected by nucleation. However, ATD(iPP) for β-nucleated grades were lower than ATD(iPP) for the nonnucleated materials. These results are in contradiction with both mechanics (Table VII) and visual observation of the DMA trace (Fig. 19). Moreover, they did not reflect the higher amount of loss energy of β-nucleated structures over their nonnucleated homologs (about +25%) and the higher intensity of the matrix relaxations for the β-iPP/EPR (Fig. 20). The usual determination of ATD(iPP) was, therefore, not suited, as a consequence of (1) some overlapping between the β-relaxation and the α_c-relaxation peaks and (2) mismatches in height between the delimiting minima of ATD(iPP). Indeed, whereas the intensities of low temperature minima ($T \sim -30$°C) were about 0.02 for both series, those related to the high temperature minima ($T \sim 24$°C) occurred at different amplitude levels (about 0.035 for the nonnucleated grades, about 0.055 for the β-nucleated ones).

More generally, the determination of meaningful ATD values will be difficult as soon as the materials to compare do not exhibit a rather homothetic DMA trace. With the exception of the β-nucleated series, this prerequisite was roughly assured up to now.

A solution to overcome this critical issue could be to set other peak limitations than two consecutive mimina. Getting an incontestable base line is, however, difficult. A method that works quite well in cases such as those depicted before is shown in Figure 21. It consists of defining the baseline as a constant independent of the temperature. This constant is equal to $\min_{\tan\delta}$ (with $\min_{\tan\delta}$, the minimum of intensity re-

TABLE VII
Impact Fracture Resistances at 23°C ($NIS_{23°C}$) and Relaxation Strengths of Rubber Phase [ATD(EPR)] and matrix [ATD(iPP)] for Nonnucleated and β-Nucleated Reactor iPP/EPR with Identical Matrix MFR and Different Rubber Intrinsic Viscosities

IV	1.7	2.1	2.7	3	3.9	4.7	6	dl/g
$NIS_{23°C}$—nonnucl.	4.5	6	7.7	9.4	10.8	11.8	12.9	kJ/m^2
ATD(iPP)—nonnucl.	0.310	0.314	0.299	0.279	0.281	0.254	0.240	rel. units
ATD(EPR)—nonnucl.	0.360	0.394	0.402	0.433	0.458	0.498	0.520	rel. units
$NIS_{23°C}$—β-nucl.	7.1	7.9	8.8	12.1	14.3	15.9	16.4	kJ/m^2
ATD(iPP)—β-nucl.	0.241	0.279	0.286	0.262	0.257	0.273	0.247	rel. units
ATD(EPR)—β-nucl.	0.389	0.397	0.406	0.445	0.468	0.502	0.531	rel. units

Note that ATD(EPR) for both nonnucleated and β-nucleated grades are nearly equal for a given IV contrarely to ATD(iPP). In this case, ATD(iPP) do not correlation with material ranking (in terms of fracture toughness).

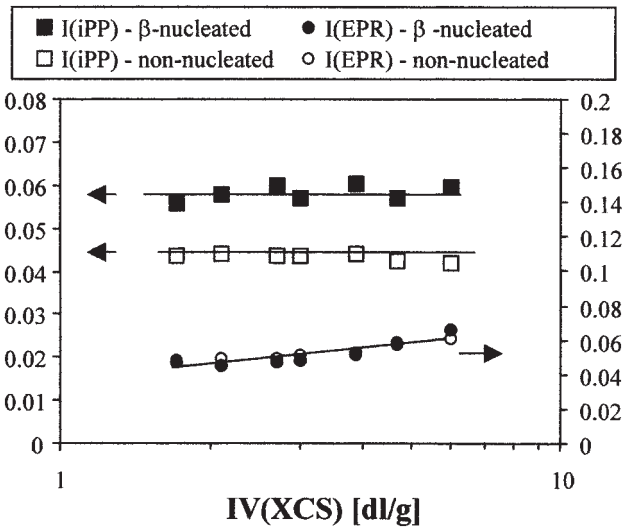

Figure 20 Intensities [i.e., height of max (tan δ)] of the rubber and matrix relaxations [resp. I(EPR) and I(iPP)] plotted vs the logarithm of the EPR intrinsic viscosity (IV) for a series of nonnucleated and β-nucleated iPP/EPR blends where the IV of the dispersed phase have been varied selectively all other parameters (inclusive matrix MFR) having been kept constant.

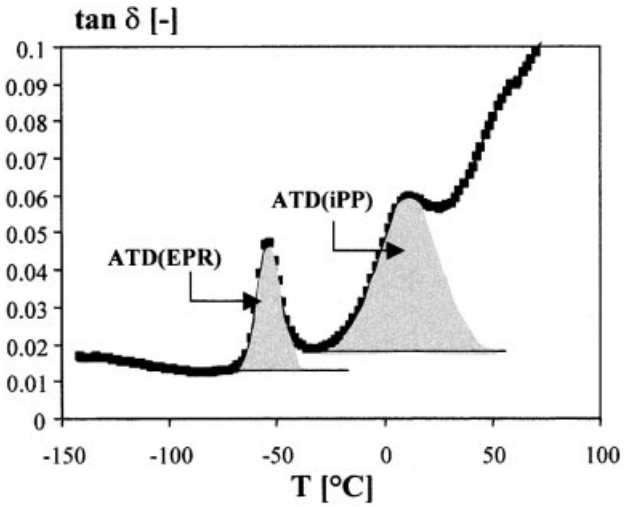

Figure 21 Alternative procedure to evaluate the strengths of the rubber, ATD(EPR), and matrix, ATD(iPP), relaxations.

corded near to the considered relaxation) and extrapolate the relaxation peak up to this minimum. The obtained values correlate with micromechanical data as revealed Table VIII: the higher mobility (as thus the higher fracture resistance) of β-nucleated materials are reflected by corrected ATD(iPP) values.

As a consequence, a minimum knowledge about the materials in investigation is required to guarantee adequate interpretation and data reduction of DMA traces.

CONCLUSION

Potential and limits of dynamic mechanical analysis (DMA) as a tool for fracture resistance evaluation of isotactic polypropylenes and their polyolefin blends have been highlighted. A minimum of information about the materials under investigation is a prerequisite to interpretate the DMA traces in the right way, because several independent parameters influence peak relaxations. For iPP/EPR blends, we have, for example, pointed out the combined effect of M_w and rubber amount on the strength of the rubber relaxation. For iPP homopolymers, the influence of the catalyst system is obvious. As a practical consequence, mechanical performances of unknown materials cannot be predicted using DMA as unique test method.

Moreover, although DMA is, in general, a powerful method to rank materials in term of toughness care should be taken (1) with nucleated materials (where both intensity and strength of molecular relaxations should be taken into account in material evaluation), and (2) with visbroken grades (where the intensity and strengths of the relaxations are not affected by peroxide degradation). Except for these cases, the strengths of the principal or secondary molecular relaxation evaluated by DMA and the Charpy impact

TABLE VIII
Impact Fracture Resistances at 23°C ($NIS_{23°C}$) and Corrected Relaxation Strengths of Rubber Phase [ATD(EPR)] and Matrix [ATD(iPP)] for Nonnucleated and β-Nucleated Reactor iPP/EPR with Identical Matrix MFR and Different Rubber Intrinsic Viscosities

IV	1.7	2.1	2.7	3	3.9	4.7	6	dl/g
$NIS_{23°C}$—nonnucl.	4.5	6	7.7	9.4	10.8	11.8	12.9	kJ/m^2
ATD(iPP)—nonnucl.	0.87	0.84	0.862	0.722	0.674	0.578	0.546	rel. units
ATD(EPR)—nonnucl.	0.482	0.526	0.562	0.562	0.638	0.64	0.712	rel. units
$NIS_{23°C}$—β-nucl.	7.1	7.9	8.8	12.1	14.3	15.9	16.4	kJ/m^2
ATD(iPP)—β-nucl.	1.488	1.486	1.53	1.408	1.51	1.568	1.200	rel. units
ATD(EPR)—β-nucl.	0.478	0.516	0.57	0.636	0.624	0.636	0.732	rel. units

Note that ATD(EPR) for both nonnucleated and β-nucleated grades are nearly equal for a given IV contrarely to ATD(iPP). In this case, ATD(iPP) correlation with material ranking (in terms of fracture toughness).

toughness correlate quantitatively when all the grades of a series under investigation (with one of the parameter either "rubber M_w" or "rubber content" hold constant) exhibit unstable crack propagation. When changes in the macroscopic mode of fracture or in blend morphology occur, only qualitative correlations remain possible.

Overall, DMA appears to be a rather sound method for mechanical characterization of iPP and its blends. Judiciously used in combination with other relevant measurements, it constitutes an outstanding research and quality control tool.

The authors would like to thank their colleagues B. Knogler, J. Fiebig, W. Pirgov, N. Hafner, and J. Wolfschwenger from Borealis GmbH Austria for having provided some of the raw data for this work.

References

1. Jafari, S. H.; Gupta, A. K. J Appl Polym Sci 2000, 78, 962.
2. Lotti, C.; Correa, C. A.; Canevarolo, S. V. Mater Res 2000, 3, 37.
3. Järvelä, P.; Shucai, L.; Järvelä, P. J Appl Polym Sci 1996, 62, 813.
4. Lovisi, H.; Tavares, M. I. B.; da Silva, N. M.; de Menezes, S. M. C.; de Santa Maria, L. C.; Coutinho, F. M. B. Polymer 2001, 42, 9791.
5. Woo, L.; Westphal, S.; Ling, M. T. K. Polym Eng Sci 1994, 34, 420.
6. Jain, A. K.; Nagpal, A. K.; Singhal, R.; Gupta, N. K. J Appl Polym Sci 2000, 78, 2089.
7. Ramsteiner, F. Kunststoffe 1983, 73, 148.
8. Karger-Kocsis, J.; Kuleznev, V. N. Polymer 1982, 23, 699.
9. Kisbenyi, M.; Birch, M. W.; Hogkinson, J. M.; Williams, J. G. Polymer 1979, 20, 1289.
10. Vincent, P. I. Polymer 1974, 15, 111.
11. Karger-Kocsis, J.; Kiss, L. Polym Eng Sci 1987, 27, 254.
12. Grein, C.; Grein, C.; Béguelin, P., Plummer, C. J. G.; Kausch, H.-H.; Tézé, L.; Germain, Y. In Fracture of Polymers, Composites and Adhesives; Williams J. G., Pavan, A., Eds.; ESIS Pulication 27; Elsevier Science: UK, 2000; p 319.
13. Sepe, M. P. Dynamical Mechanical Analysis for Plastic Engineering; PDL Handbook Series: Norwich, NY, 1998.
14. Read, B. E. Polymer 1989, 30, 1439.
15. Boyd, R. H. Polymer 1986, 26, 323.
16. Fiebig, J.; Gahleitner, M.; Paulik, C.; Wolfschwenger, J. Polym Test 1999, 18, 257.
17. Frontini, P. M.; Fave, A. J Mater Sci 1995, 30, 2446.
18. Alberola, N.; Fugier, M.; Petit, D.; Fillon, B. J Mater Sci 1995, 30, 860.
19. Alberola, N.; Fugier, M.; Petit, D.; Fillon, B. J Mater Sci 1995, 30, 1187.
20. Ferrer-Balas, D.; Maspoch, D.; Ll.; Martinez, A. B.; Santana, O. O. Polymer 2001, 42, 2001.
21. Perkins, W. G. Polym Eng Sci 1999, 39, 2445.
22. Walker, I.; Collyer, A. A. In Rubber Toughened Engineering Plastics; Collyer, A. A., Ed.; Chapman & Hall: London, 1994; p 29.
23. Starke, J. U. ;Michler, G. J.; Grellmann, W.; Seidler, S.; Gahleitner, M.; Fiebig, J.; Nezbedova, E. Polymer 1998, 39, 75.
24. Grellmann, W.; Seidler, S.; Jung, K.; Kotter, I. J Appl Polym Sci 2001, 79, 2317.
25. Grein, C.; Bernreitner, K.; Gahleitner, M.; Hauer, A.; Neißl, W. J Appl Polym Sci 2003, 87, 1702.